A frontier in the understanding of synaptic plasticity: Solving the structure of the postsynaptic density

Matthew G. Gold

The postsynaptic density (PSD) is a massive multi-protein complex whose functions include positioning signalling molecules for induction of long-term potentiation (LTP) and depression (LTD) of synaptic strength. These processes are thought to underlie memory formation. To understand how the PSD coordinates bidirectional synaptic plasticity with different synaptic activation patterns, it is necessary to determine its three-dimensional structure. A structural model of the PSD is emerging from investigation of its molecular composition and connectivity, in addition to structural studies at different levels of resolution. Technical innovations including mass spectrometry of cross-linked proteins and super-resolution light microscopy can drive progress. Integrating different information relating to PSD structure is challenging since the structure is so large and complex. The reconstruction of a PSD subcomplex anchored by AKAP79 exemplifies on a small scale how integration can be achieved. With its entire molecular structure coming into focus, this is a unique opportunity to study the PSD.

DOI 10.1002/bies.201200009

Department of Neuroscience, Physiology and Pharmacology, University College London, London, UK

Corresponding author:
Matthew G. Gold
E-mail: m.gold@ucl.ac.uk

Abbreviations:
AMPAR, AMPA-type glutamate receptor; **CaM,** calmodulin; **CaMKII,** Ca^{2+}/CaM-dependent protein kinase II; **EM,** electron microscopy; **LTD,** long-term depression; **LTP,** long-term potentiation; **MAGUK,** membrane-associated guanylate kinase; **MS,** mass spectrometry; **NMDAR,** NMDA-type glutamate receptor; **PALM,** photo-activated localisation microscopy; **PKA,** protein kinase A; **PP2B,** protein phosphatase 2B; **PSD,** postsynaptic density; **STORM,** stochastic optical reconstruction microscopy.

Keywords:
mass spectrometry; memory; postsynaptic density; structure; synaptic plasticity

Introduction

How does the brain encode memories? Each new experience leads to a complex pattern of electrochemical communication between subpopulations of neurons that are interconnected by synapses. A popular theory is that changes in the strength of these synapses are an important component of memory formation [1]: cellular protocols dictate the direction of synaptic plasticity depending on the stimulation pattern of each synapse. Influential supporting evidence for this theory is that different artificial stimulation protocols lead to either strengthening or weakening of synapses between CA3 and CA1 neurons in the hippocampus. High-frequency tetanic stimulation of Schaffer collateral axons projected by CA3 neurons leads to an increase in the excitatory postsynaptic potential elicited in CA1 neurons with which they form synapses. This effect lasts for several hours and is known as long-term potentiation (LTP), a term coined to describe a similar phenomenon in excitatory connections on hippocampal granule cells [2]. Conversely, low-frequency stimulation leads to long-lasting weakening of the same synaptic population known as long-term depression (LTD) [3]. Together, LTP and LTD at Schaffer collateral-CA1 synapses constitute the prototypical form of synaptic plasticity. The molecular basis of both LTP and LTD has been vigorously investigated on the assumption that it will uncover general mechanisms employed by neurons in modifying synaptic strength. This research has revealed that signalling in a proteinaceous specialisation of the dendritic spine called the postsynaptic density (PSD) is central to the induction of both LTP and LTD [4].

The PSD was first observed in electron micrographs as 'localised regions of thickening and increased density' [5] attached to the postsynaptic [6] membrane of excitatory synapses. The thickness of the PSD was first measured at ~50 nm by electron microscopy (EM) of isolated PSDs [7]. EM of thinly

sectioned hippocampal neurons indicates that a PSD at the head of a typical 'thin' dendritic spine is disc shaped, with a surface area of ~0.07 μm^2 and a thickness of ~25 nm [8, 9]. The PSD positions glutamate receptors across from pre-synaptic glutamate release sites, and links the receptors to intracellular signalling cascades. The structure is a locus for mutations causing neurological disease and psychiatric disorders [10], underlining its critical role in synaptic transmission and plasticity. For example mutations in the PSD scaffold proteins Shank2 [11] and Shank3 [12] are associated with Autism Spectrum Disorders, while mutations in LGI1 and ADAM22 are related to epilepsy [13]. Investigation of the molecular basis of frequency-dependent synaptic plasticity in the Schaffer collateral pathway has revealed some general mechanisms for synaptic plasticity: entry of Ca^{2+} into the PSD through NMDA-type glutamate receptors (NMDARs) is often a requirement for both LTP [14, 15] and LTD [3, 16], and trafficking and regulation of the open probability/single-channel conductance of AMPA-type glutamate receptors (AMPARs) is fundamental to changes in the strength of many types of synapse [17]. However, the field awaits a mechanism to describe how signalling molecules in the PSD can link Ca^{2+} entry to both up or down-regulation of AMPAR currents depending on the pattern of stimulation. As I shall discuss, a number of signalling proteins are thought to modify AMPAR currents [18] in response to Ca^{2+} entry. However, many different signalling molecules have been implicated, and the PSD is so complex that it is difficult to be sure which molecules constitute the 'core program' [19] for induction of synaptic plasticity.

Linus Pauling opined that 'It is structure that we look for when we try to understand anything' [20]. Structural studies have been integral to conceptual breakthroughs throughout the history of neuroscience. Examples include the development of neuron theory by Cajal on the basis of characterisation of the neuronal architecture of the brain using the Golgi method, and support for chemical transmission through resolution of the synaptic cleft by EM. Determination of the layout of ion channels and signalling molecules in the PSD at high resolution also has the potential to drive conceptual development. In this review, I shall discuss progress on four experimental branches that are necessary for a molecular reconstruction of the PSD (Fig. 1). The complexity of the structure is such that data integration and model building are crucial for progress, and these topics are also reviewed. Firstly though, I shall further consider the significance of PSD structure in research into the molecular basis of synaptic plasticity.

The molecular structure of the PSD is a blueprint for understanding synaptic plasticity

Research into the molecular basis of synaptic plasticity has converged on the regulation of AMPAR phosphorylation by enzymes that respond to postsynaptic Ca^{2+} entry. During LTP, residue Ser831 of GluR1 AMPARs is phosphorylated by Ca^{2+}/calmodulin (CaM)-dependent protein kinase II (CaMKII) and protein kinase C [21, 22], which increases single-channel conductance [23]. Ser831 phosphorylation is opposed by phosphatases [21], which are thought to include protein phosphatase 1 acting downstream of Ca^{2+}/CaM-activated protein phosphatase 2B (PP2B) [24]. PP2B also directly dephosphorylates the cAMP-dependent protein kinase A (PKA) phosphorylation site Ser845 [21] during LTD, which both decreases the open probability of AMPARs and leads to their trafficking out of the PSD. This AMPAR phosphorylation-centric model [25] of synaptic plasticity is supported by changes in hippocampal AMPAR phosphorylation in rats following inhibitory avoidance training [26].

How then can high-frequency tetanic stimulation and low-frequency stimulation lead to opposite effects when both LTP and LTD are induced by Ca^{2+}-sensitive enzymes acting downstream of postsynaptic Ca^{2+} entry? It was suggested that the direction of synaptic plasticity was dictated by the NMDA receptor subtype [27] present in a given PSD, but this has since been refuted [28]. Rather than being determined by the presence or absence of a particular protein, it is likely that spatio-temporal subtleties in Ca^{2+} signals determine the direction of plasticity. Second messengers, including Ca^{2+} and cAMP, are elevated in cellular microdomains [29, 30]; a second messenger-responsive enzyme will not be activated unless it is positioned within such a microdomain. Similarly, substrates must be in proximity to the microdomain or they will not be acted upon. Three factors that affect whether a second messenger-dependent signalling event falls within a microdomain are: (i) the size of the microdomain as determined by the signal amplitude, for example high-frequency tetanic stimulation enables maximal Ca^{2+} entry through NMDARs and thus activates signalling enzymes over a larger volume; (ii) the position of enzymes and substrates in relation to the second messenger generation/entry location, for example the anchoring protein AKAP79 (AKAP150/AKAP5) positions PKA and PP2B for bidirectional phosphoregulation of AMPAR GluR1 residue Ser845 [31, 32]; (iii) the duration of the elevation in second messenger concentration since the architecture of the signalling microdomain may itself be regulated by the second messenger [33]. Importantly, the Ca^{2+}/CaM-sensitive enzymes CaMKII and PP2B are probably positioned at different distances from the NMDAR mouth in the PSD axiodendritic axis (Fig. 2), which suggests that PP2B may be able to sense smaller quantities of postsynaptic Ca^{2+} entry. The significance of signalling enzyme targeting is underlined by many reports of protein-protein interactions critical to synaptic plasticity, including interactions that position CaMKII [34, 35]. Therefore, to understand synaptic plasticity, it is necessary to determine how the critical Ca^{2+}-sensitive signalling enzymes are positioned relative to Ca^{2+} entry points and their substrates in the PSD. Answering this question requires an accurate structural model of the PSD.

The PSD structure also provides a foundation for understanding how synaptic plasticity is expressed following induction. For example the machinery for endocytosis of AMPARs is positioned laterally to the PSD and connected to it by direct protein-protein interactions [36]. Pre-synaptic changes also contribute to the expression of synaptic plasticity [37]. The emphasis in this review is on understanding the canonical homosynaptic frequency-dependent form of synaptic plasticity in the Schaffer collateral pathway. However, PSD structure is also likely to contribute to the understanding of forms of plasticity that are pre-synaptically induced, such as in the mossy fibre pathway

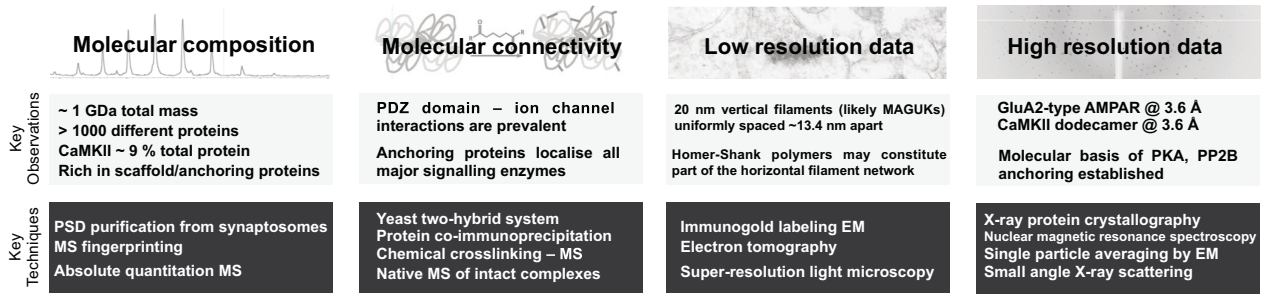

Figure 1. A multi-faceted experimental scheme for solving the structure of the PSD. Key observations and techniques are listed for four experimental branches that are enabling determination of the molecular structure of the PSD.

[38, 39], by explaining how signalling processes operate through PSD proteins that cross the synaptic cleft; and that are induced by different stimulation protocols, such as spike-timing dependent plasticity [40]. Given that it is critical to form a structural model of the PSD, the following sections describe the progress and outlook of four experimental branches that enable the molecular structure of the PSD to be pieced together (summarised in Fig. 1).

Determination of the molecular composition of the PSD is fundamental to its reconstruction

The starting point for assembling a structural model of the PSD is the identification and quantification of its constituent molecules. Methods to purify the PSD are an essential component of such research. PSD purification protocols are predominantly derived from the Whittaker synaptosome preparation [41], in which a sucrose gradient is applied to a particulate brain fraction to purify the nerve endings. PSDs can be isolated from synaptosomes by extracting the synaptic membranes with non-ionic detergent [42] such as 1% Triton X-100 [43].

The first PSD proteins were identified by biochemical characterisation of the most prominent proteins [44] following SDS-PAGE of purified PSDs, such as CaMKII [45] and the membrane-associated guanylate kinase (MAGUK) protein PSD-95 [46]. Latterly, peptide mass fingerprinting by mass spectrometry (MS) has revealed that a great diversity of different proteins are located in the PSD. For example 1,461 proteins were identified by this approach in PSDs purified from human neocortex [10]. Comparison of different proteomic efforts shows that more than 400 proteins are regularly identified across different PSD preparations [47] by MS fingerprinting. Membrane receptors and channels, proteins involved in signalling by protein phosphorylation and scaffold and anchoring proteins are well represented in the PSD proteome [48]. Within the scaffold protein subset, proteins containing PDZ domains are a hallmark of the PSD.

The presence of a large subset of mitochondrial proteins in the 'PSD' proteome [48] is cautionary. While identification of PSD proteins by MS fingerprinting is extremely sensitive, the efficacy of the approach is limited by the quality of the initial PSD purification. Limitations of the current PSD purification method include: cellular contaminants including mitochondria, loss of PSD proteins in high concentrations of detergent during the membrane extraction phase and presence of presynaptic proteins via physical association with PSD proteins that bridge the synaptic cleft. PSD purification methods are essentially unchanged in over 30 years [10, 42], so there may be scope for improvement in this area.

Although the number of proteins identified in the PSD is daunting, the dimensions of the PSD limit the diversity of proteins that can be accommodated within it. The Matthew's coefficient V_M, which is used to assess the solvent content of protein crystals [49], can be used to estimate the mass of the PSD from its volume. The most commonly observed values for V_M in protein crystals cluster around 2.15 $Å^3$/Da, which corresponds to 43% solvent content. If we assume that the PSD is closely packed to the same degree, for a typical PSD with a volume of ~2 $GÅ^3$ the estimated protein mass is 0.93 GDa. This is consistent with a mass of ~1 GDa measured by scanning EM of purified PSDs [50], suggesting that ~15–20,000 polypeptide chains make up a single PSD.

Some proteins are present at a high-copy number in the PSD, which simplifies the problem. The MS 'absolute quantification' method, which uses labelled synthetic peptides as internal standards, has been utilised to determine the concentrations of a selection of proteins in PSDs purified from rat forebrain [51]. CaMKII isoforms were found to constitute ~9% of total PSD protein by this method [51]. These concentrations can be used to estimate the copy numbers of different proteins in the PSD – approximately 5,600 copies in the case of CaMKII [48, 51]. Scaffold proteins are also over-represented, with ~300*PSD-95, 360*SynGAP, 150*Shank isoforms and 20*AKAP79 per PSD [48]. Copy numbers of PSD proteins determined by both quantitative gel electrophoresis [50] and a GFP-based calibration technique [52], are generally consistent with these numbers. Comparative analysis using cleavable isotope-coded affinity tag MS shows that there are regional differences in the protein make-up of the PSD. For example SynGAP and CaMKII are expressed approximately five-fold more highly in PSDs purified from forebrain compared to cerebellum [51]. Isobaric tagging MS has enabled comparative analysis of protein expression and phosphorylation in the murine cortex, midbrain, cerebellum and hippocampus [53]. This revealed that protein phosphorylation is relatively higher in the hippocampus. Regional differences in PSD composition reflect regional variations in the molecular mechanisms underlying synaptic plasticity [18]. Nevertheless, the majority of proteins compared in forebrain and cerebellum were not expressed at significantly different levels [51]. This

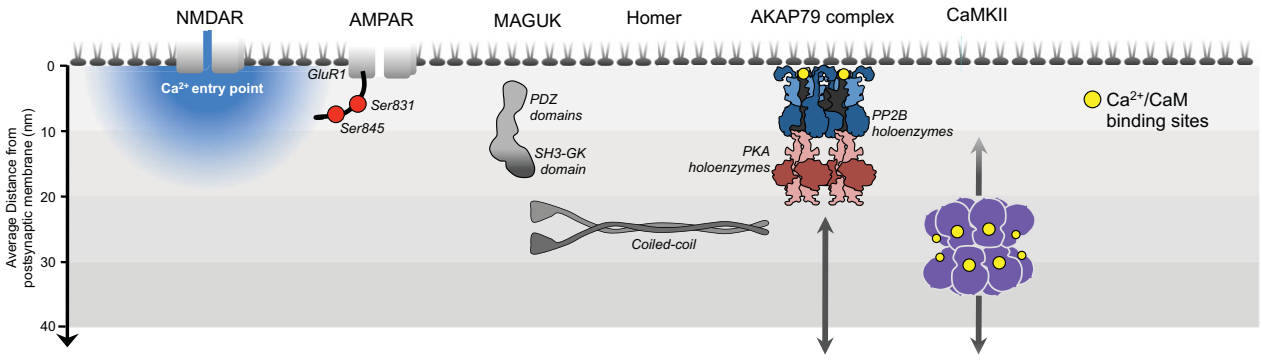

Figure 2. Laminar organisation of PSD signalling molecules involved in AMPAR phosphoregulation. Approximate distances are illustrated from the internal edge of the postsynaptic bilayer in the axodendritic axis. Distances are derived from immuno-EM [67, 70, 105] studies, with the exception of the AKAP79 complex, whose position is approximated on the basis that the N-terminus of AKAP79 binds to membrane phospholipids [106]. Protein outlines of a MAGUK protein (SAP97), Homer, the AKAP79 complex and the CaMKII holoenzyme are approximately to scale [54, 68, 72, 84]. The lateral organisation of proteins in the diagram is not intended to be realistic.

suggests that PSDs perform broadly similar functions throughout the brain.

Developing methods are useful for determining the stoichiometries of protein subcomplexes present in the PSD. Mass calculation of intact protein complexes by native MS can be sufficiently accurate to enable unambiguous stoichiometric assignment. A PSD subcomplex nucleated by AKAP79 was measured at 466 kDa by this method, indicating that the complex consists of two copies of AKAP79, two copies of CaM, four copies of PKA and four copies of PP2B [54]. The single-molecule pull-down assay [55], which relies on fluorescence microscopy and can be applied in vivo, is also likely to be useful in determining the exact stoichiometries of PSD subcomplexes. Continued characterisation of the PSD proteome by quantitative techniques will facilitate model building by establishing how many copies of each PSD protein must be positioned within global structural models.

The molecular connectivity of the PSD limits how its molecular components can be assembled

Order in the PSD arises from specific interactions between surfaces presented by its constituent molecules. Determining these interactions is an important step in reconstructing the PSD. Protein-protein interactions were initially identified in the PSD by yeast two-hybrid screening. Examples are the interaction between the C-terminus of NR2B-type glutamate receptors and the second PDZ domain of PSD-95 [56], and the AKAP79-PP2B interaction [57]. SynGAP was identified by this approach using the third PDZ domain of a MAGUK protein as bait [58].

The yeast two-hybrid system is less well suited to identifying lower affinity interactions found in multi-protein complexes in which each protein simultaneously interacts with multiple proteins. These interactions are a feature of the PSD. An alternative approach is to immunoprecipitate a given PSD protein and characterise its co-precipitants. For example a MAGUK-associated signalling complex containing approximately 100 proteins can be purified using either the last six C-terminal amino acids of NR2B as an affinity ligand, or with anti-NR2B antibodies [59, 60]. The co-immunoprecipitating proteins are likely to be in proximity to each other. Immunoprecipitations are often performed using whole brain lysate. In the case of NMDAR-associated proteins, care must be taken to distinguish proteins in complex with synaptic and extra synaptic NMDARs, which have important functional differences [61]. Variations on the co-immunopreciptation strategy include the use of low-background tandem affinity purifications, such as was used to determine PSD proteins in complex with PSD-95 [62].

Co-immunoprecipitation does not distinguish direct and indirect interactions. Follow-up experiments with purified protein and methods to quantify binding thermodynamics such as isothermal titration calorimetry can differentiate between the two interaction modes. However, weaker direct PSD interactions may still evade detection outside of the context of the PSD. A novel approach is peptide fingerprinting of cross-linked peptides following trypsinisation of cross-linked protein complexes [63]. In this method, protein complexes are chemically cross-linked with a cross-linker of a set linker length prior to trypsinisation. If the spectrometer detects a molecule corresponding to peptides from two different proteins bridged by the cross-linker this indicates that the cross-linked residues from the two proteins are within a certain distance in the native structure [64, 65]. The approach has been applied on a small scale to identify a homomeric dimerisation site in AKAP79 in proximity to residues 328–333 [54]. It could be applied on a larger scale to map interactions in PSD subcomplexes or within an intact PSD. Analysis of fragmentation patterns in native MS experiments is another avenue for determining the connectivity of proteins within multi-protein complexes [66]. These novel MS-centric approaches are likely to complement the current methods for determining PSD connectivity in the future.

Electron and super-resolution light microscopy are revealing PSD structure at low resolution

EM continues to play an important role in interrogating global PSD structure, following the first imaging of the PSD by this method in the 1950s. Structures as small as 3–4 nm in

diameter can be resolved within 1–1.5 nm-thick virtual sections following electron tomography of dendritic spines [67]. This approach reveals that 'vertical' filaments approximately 5 nm wide and 20 nm long are uniformly spaced throughout the PSD with a nearest neighbour distance of 13.4 nm. At this spacing roughly 400 vertical filaments punctuate a PSD 400 nm in diameter. Comparison with single-particle images of the MAGUK protein SAP97 by EM indicates that the vertical filaments are approximately the length of an extended MAGUK protein [68]. Immunogold labelling studies, and the patchy loss of vertical filaments [69] in PSD-95 knockdown neurons, suggests that MAGUK proteins with their N-termini proximal to the membrane correspond to vertical filaments. Laminar organisation is a general feature of the PSD, with the peak concentrations of different proteins at different distances from the membrane [70] (Fig. 2). Classification of AMPA and NMDA-type glutamate receptors as well as horizontal and vertical filaments has enabled construction of a model of the core filamentous structure of the PSD [67]. PSD horizontal filaments fall into two morphological classes, which may correspond to the scaffold proteins GKAP and Shank [67]. Negative stain EM demonstrates that Shank3 is filamentous [71] and that a 1:1 mixture of purified Homer1b and Shank1C polymerises to form a network structure. Therefore, Homer and Shank may constitute an important component of the horizontal filament network [72]. Immunogold labelling also reveals that the endocytic machinery (AP-2, clathrin and dynamin) is sequentially organised laterally to the PSD in dendritic spines [73]. This suggests that receptors decouple from the PSD prior to endocytosis in an adjacent functional domain. Additional ultrastructural features, including filaments linking the PSD and actin cytoskeleton [74], are visible following high-pressure freezing. This approach likely produces more realistic images than normal aldehyde fixation.

'Super-resolution' light microscopy techniques, based on single-molecule detection, are contributing to investigations of PSD ultrastructure [75, 76]. Spatial resolution approaching 20 nm has been achieved using photo-activated localisation microscopy (PALM) [76] and the related stochastic optical reconstruction microscopy (STORM) [77]. The axial distributions of synaptic proteins measured using STORM [77] are broadly consistent with prior immuno-EM studies [70]. Two advantages of PALM/STORM compared to EM are the ability to observe dynamics and to simultaneously visualise multiple molecules. These were showcased in a recent study of actin spine dynamics [78]. Quantum dot imaging is another powerful method for following in vivo dynamics at high resolution, for example this approach has been applied to show that GluR1 AMPAR mobility is restricted in active synapses [79]. Super-resolution light microscopy, in tandem with two and three-dimensional EM approaches, should enable a three-dimensional map of constituent proteins to be assembled at lower resolution.

Analysis of purified protein substructures reveals PSD structural features at high resolution

A low-resolution model of the PSD could be drawn up using information gathered by the techniques outlined in the three preceding sections. In order to add molecular detail, high (~3 Å or better) resolution structural information is required. Progress has been made in determining high-resolution structures of the proteins that comprise the AMPAR phosphorylation-centric model of bidirectional synaptic plasticity [49]. The crystal structure of the transmembrane and extracellular domains of the GluA2 AMPAR has been determined [80]. Crystal structures of the ligand-binding domains of the NMDAR [81] provide insights into the arrangement of the receptor subunits. The structure of the NMDAR pore, which corresponds to the entry sites of Ca^{2+} into the PSD, is yet to be determined. The three-dimensional structures of the globular signalling enzymes that control the phosphorylation state of AMPA receptors have been solved [82–85]. These include a crystal structure of the majority of the PKA holoenzyme in which the cAMP-binding domains of the RII subunit form multiple contact points with the catalytic subunit [82]; and the CaMKII holoenzyme structure showing that the CaM-binding sites are inaccessible in the auto inhibited kinase dodecamer [84].

High-resolution structures detailing PSD protein-protein interactions are particularly constructive. MAGUK family proteins, which simultaneously interact with multiple integral membrane proteins via PDZ domain interactions, are essential for the structural integrity of the PSD [69]. The molecular basis of selective PDZ domain interactions has been established [86]. Further important interactions that have been determined at high resolution include the anchoring mechanisms for PKA and PP2B. AKAP79 associates with the N-terminal dimerisation and docking (D/D) domain of PKA RII subunits through a hydrophobic interface presented by an amphipathic helix that is conserved in the AKAP family [87, 88]. An additional structural motif in AKAP79 simultaneously anchors two copies of PP2B [54]. The anchoring protein contributes the central strand of a three-stranded β-sheet, in which the outer β-strands correspond to β-14 strands of PP2B catalytic A subunits [89, 90]. It can be difficult to obtain high-resolution structures of full-length anchoring and scaffold proteins, which are generally too large for nuclear magnetic resonance and lack tertiary structure elements that favour crystallisation. Crystallising protein complexes is also challenging. In such cases complementary techniques including small angle X-ray scattering [84] and single-particle averaging by EM can generate electron density maps at a resolution that is at least sufficient to locate protein subdomains [68]. These approaches may also reveal large-scale dynamics, for example between the PDZ and SH3-GK domains of SAP97 [68].

For PSD proteins where no high-resolution structure is available, structure can potentially be modelled by homology to proteins of known structure. If not, application of the battery of approaches detailed above is likely to yield useful information.

Integration of PSD structural data into inclusive models will present functional insights

Francis Crick thought that 'A good model... should serve to unite evidence from several different approaches' [91]. In the case of the PSD, information concerning its structure contin-

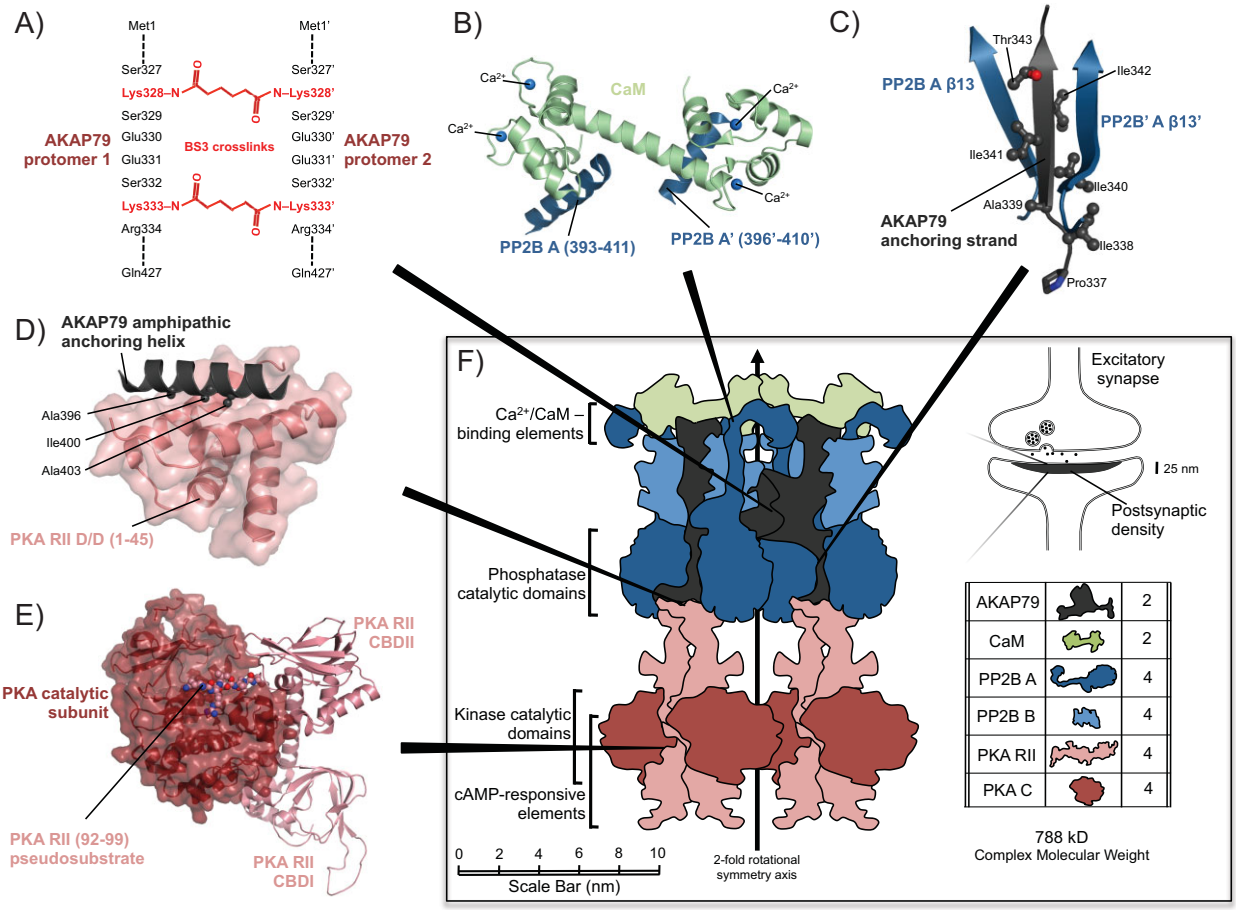

Figure 3. Structure of the postsynaptic AKAP79 signalling complex. **A:** AKAP79 homomeric cross-linking sites indicate that AKAP79 forms a parallel dimer and that there is likely to be a dimerisation site in proximity to residues 328–333 [54]. **B:** Crystal structure of a complex between PP2B (blue) and CaM (green; PDB ID 2R28) [107]. **C:** Crystal structure of the AKAP79 phosphatase anchoring peptide (grey) in complex with two PP2B A subunits (blue; PDB ID 3LL8) [90]. **D:** Molecular basis of PKA anchoring to AKAP79. AKAP79 presents an amphipathic helix (grey) for interaction with a hydrophobic face on the PKA RII D/D domain (pink; PDB ID 2IZX) [87]. **E:** Crystal structure of a complex between PKA RII (light red) and C (dark red) subunits (PDB ID 2QVS) [82]. **F:** The stoichiometry of an intact 2*AKAP79:2*CaM:4*PP2B:4*PKA complex was determined by native mass spectrometry [54]. In the central model, protein outlines and the scale bar are derived from crystal structures with the exception of AKAP79, the C-terminal 150 amino acids of PP2B A and the linker (residues 46–90) between the PKA RII D/D and cAMP-binding domains.

ues to accumulate from different approaches. Perhaps the greater challenge is uniting the data into a comprehensive model. The postsynaptic AKAP79 signalling complex [31, 32] exemplifies on a relatively small scale how different types of structural information can be integrated. In this case we know that its interacting proteins include PP2B, PKA and CaM; the location of its dimerisation site (Fig. 3A); the structures of associated proteins PKA, PP2B and CaM at high resolution; and the structures of interfaces between PP2B-CaM (Fig. 3B), AKAP79-PP2B [89] (Fig. 3C), AKAP79-PKA [87, 88] (Fig. 3D) and PKA RII and C subunits (Fig. 3E) at high resolution. Given the stoichiometry of the complex, which was measured using native MS [54], we can draw up the model shown in Fig. 3F. The model suggests that the complex is approximately 20 nm in its longest dimension, and likely spans the depth of the PSD (Fig. 2). It also suggests that the Ca^{2+}/CaM-sensitive elements of AKAP79 and PP2B are proximal to the membrane, whereas the cAMP-binding elements of PKA are distal to the membrane, with the catalytic sites of anchored enzymes PKA and PP2B in-between.

Evidence from different approaches would enable the model to be improved: If an electron density map of the complex could be determined this would allow docking of the respective crystal structures, as has been achieved with other multi-protein complexes [92]. Absolute quantitation MS estimated that approximately 20 copies of AKAP79 are present per PSD [51]; determination of the location of these complexes within the PSD by a technique such as PALM would enable extension of the model to the scale of the PSD. Finally AKAP79 is known to interact with MAGUK proteins [93], but this interaction is poorly characterised. With the molecular basis of this interaction in hand, the model could be integrated with structural models of MAGUK proteins in the PSD. Given that the AKAP79 signalling complex constitutes 788 kD, the presence of ~20 copies of AKAP79 per PSD, and an estimated mass of ~1 GDa per PSD, the AKAP79

Table 1. Bioinformatics for integrating data to develop structural PSD models

Category	Tool/resource	Capabilities
Databases	G2Cdb	The Genes to Cognition consortium's database includes proteins identified by mass spectrometry in complex with the mouse NMDA receptor, present in the mouse postsynaptic proteome and present in PSDs isolated from human neocortex [10]
	STRING	Extensive database of known and predicted protein interactions [94]
	wwPDB	The Worldwide Protein Data Bank consists of the major international organisations for archiving macromolecular structural data, including the RCSB PDB. The EM Data Bank is to join the archive in 2012 [95]
Utilising atomic coordinates and electron density maps	Chimera	Extensible program for visualisation, analysis and editing of molecular structures, well suited to handling supramolecular assemblies and manually positioning crystal structures in electron density maps [96]
	CCP4 suite	Includes programs for atomic model building (Coot) and exploration of macromolecular interfaces, surfaces and assemblies (PDBePISA) [97]
	NORMA	Automated flexible fitting of high-resolution protein structures into electron-microscopy-derived electron density maps [98]
Physiological modeling	CellDesigner	Models of gene-regulatory and biochemical networks, based upon differential equations, are stored using the versatile Systems Biology Markup Language (SBML). Provides support for graphical model construction [100]
	NEURON	Enables kinetic modelling of ion concentrations, membrane voltage, and ion channels in compartmentalised neurons [109]

Examples of freely available tools and resources are listed in three categories. Tools for physiological modelling and deep curation of protein-protein interactions were recently subject to an exhaustive review [108].

signalling complex may contribute as much as ~1.6% of the total mass of the PSD. Reconstructing the PSD from discrete PSD subcomplexes such as the AKAP79 complex is one way to make PSD complexity more manageable.

Bioinformatics tools and resources can facilitate PSD model building (Table 1). The Genes to Cognition server details the content of different PSD proteomes and PSD subcomplexes [10], and public databases of mammalian protein-protein interactions include the STRING database [94]. The worldwide databank (wwPDB) is valuable for sharing larger models of PSD structure that incorporate data collected using EM [95]. Freely available programs for docking crystal structures into electron density maps [96–98] can assist construction of these models. There is a general trend in molecular biology from reductionism towards synthesis [99] reflected in the burgeoning field of systems biology. Signalling in the PSD is an appropriate subject for systems biologists, since the field is at the point where many different signalling molecules have been implicated but how they function together is poorly understood.

Computational modelling is an integral part of systems biology and the field is being driven by the development of new programs for modelling cellular systems [100]. However, the most advanced network models will fail to reveal the underlying biology unless they closely resemble the structures that determine the attributes of their functional networks [101]. Therefore, PSD structure can serve as a template for development and analysis of dynamic models of PSD signalling. Dynamics are an important consideration when constructing PSD structural models. Many proteins translocate into and out of the PSD, including AKAP79 [102], and dynamics within the PSD must also be considered [103]. It is likely that PSD horizontal and vertical filaments provide a framework for signalling enzymes of relatively greater mobility. The rearrangement of signalling microdomains over time following Ca^{2+} entry through NMDARs may reposition the key signalling enzymes CaMKII and PP2B in relation to critical substrates such as AMPARs. The best dynamic models of PSD signalling will also account for the effects of changes in membrane potential [101], such as depolarisation-induced release of NMDAR Mg^{2+}block [104]. Better structural models of the PSD should also provide insight into how mutations of PSD proteins pathologically affect synaptic signalling [11, 12].

It should be acknowledged that there are limitations to research targeted at PSD structure. PSDs are not truly unitary, as demonstrated by the heterogeneity in the composition of cerebellar and forebrain PSD preparations [51]. Since the Schaffer collateral pathway is the canonical pathway for synaptic plasticity, it is logical to focus studies of PSD structure on the PSD located in the dendritic spines of CA1 neurons. It would be particularly helpful to have quantitative proteomic information relating to this PSD type. As discussed, PSD structure is dynamic [33, 78, 79, 102, 103]. One solution to this complication is to attempt to 'capture' the PSD in different structural states, for example before and after prolonged Ca^{2+} elevation.

Finally, one must consider what level of accuracy is necessary for structural models to become functionally useful. Francis Crick provided this scientific parable in criticising a rival's model: 'Why then was his model of so little use? . . .The reason is that his model did not approximate the real thing closely enough' [91]. Schematic and topographic models that are commonly presented in relation to PSD function tend to bear little similarity to realistic dimensions and often deal with only a selection of signalling molecules. Such models are likely to fall into the Crickian category of 'existence proofs' that do not lead to the generation of testable theories [91]. We should continue to improve models that attempt to incorporate all PSD molecules in three dimensions until they are 'close enough' to reality to generate hypotheses that lead to deeper functional understanding. Given the progress of research in

the four areas described in this review, this moment could soon be upon us.

Conclusions

Evidence from four experimental branches is bringing the molecular structure of the PSD into focus. MS fingerprinting and quantitative analysis of PSD proteomes has revealed that, although a great diversity of proteins are accommodated within the PSD, some proteins are present at very high-copy numbers. Novel MS approaches are enabling a shift to a quantitative description of PSD composition. More systemic analysis of protein-protein interactions by MS analysis of cross-linked protein complexes is set to complement current approaches to characterising PSD protein-protein interactions. Structural proteins have been tentatively assigned to filaments running vertically and horizontally through the PSD and PALM/STORM will accelerate characterisation of the PSD ultrastructure at lower resolution. High-resolution crystal structures have been determined for several proteins with key roles in synaptic plasticity such as the NMDAR and CaMKII. High-resolution structures of PSD subcomplexes are very constructive, and progress is being made in this direction assisted by docking of crystal structures in electron density maps generated by single-particle averaging cryo-EM and small-angle X-ray scattering. Development of programs that enable dynamic systems biology modelling of complex signalling networks will aid integration of PSD structural data and the development of new theories to explain the molecular basis of synaptic plasticity.

As our understanding of the molecular structure of the PSD improves, it is likely to reveal mechanisms that provide deeper explanations of molecular processes at the synapse. Most significantly the structure provides a framework for understanding signalling in the induction of bidirectional synaptic plasticity, which is thought to enable information storage in the brain. Piecing together PSD structure is a challenge that should appeal to structural biologists who are redirecting their research towards the study of multi-protein complexes [101]; and to systems biologists looking to model complex signalling networks of profound functional importance. The field is at a transition point, with different types of structural data approaching synthesis: this is an exciting time to be involved in structural biology of the PSD.

Acknowledgments

Thanks go to Emily Jones and the anonymous reviewers for their critical appraisal of the manuscript. MGG is a Sir Henry Wellcome Postdoctoral Research Fellow.

References

1. **Bienenstock EL**, **Cooper LN**, **Munro PW.** 1982. Theory for the development of neuron selectivity: orientation specificity and binocular interaction in visual cortex. *J Neurosci* **2**: 32–48.
2. **Bliss TV**, **Lomo T.** 1973. Long-lasting potentiation of synaptic transmission in the dentate area of the anaesthetized rabbit following stimulation of the perforant path. *J Physiol* **232**: 331–56.
3. **Dudek SM**, **Bear MF.** 1992. Homosynaptic long-term depression in area CA1 of hippocampus and effects of *N*-methyl-D-aspartate receptor blockade. *Proc Natl Acad Sci USA* **89**: 4363–7.
4. **Kerchner GA**, **Nicoll RA.** 2008. Silent synapses and the emergence of a postsynaptic mechanism for LTP. *Nat Rev Neurosci* **9**: 813–25.
5. **Palay SL.** 1956. Synapses in the central nervous system. *J Biophys Biochem Cytol* **2**: 193–202.
6. **Palay SL.** 1958. The morphology of synapses in the central nervous system. *Exp Cell Res* **14**: 275–93.
7. **Carlin RK**, **Grab DJ**, **Cohen RS**, **Siekevitz P.** 1980. Isolation and characterization of postsynaptic densities from various brain regions: enrichment of different types of postsynaptic densities. *J Cell Biol* **86**: 831–45.
8. **Harris KM**, **Jensen FE**, **Tsao B.** 1992. Three-dimensional structure of dendritic spines and synapses in rat hippocampus (CA1) at postnatal day15 and adult ages: implications for the maturation of synaptic physiology and long-term potentiation. *J Neurosci* **12**: 2685–705.
9. **Dosemeci A**, **Tao-Cheng JH**, **Vinade L**, **Winters CA**, et al. 2001. Glutamate-induced transient modification of the postsynaptic density. *Proc Natl Acad Sci USA* **98**: 10428–32.
10. **Bayes A**, **van de Lagemaat LN**, **Collins MO**, **Croning MD**, et al. 2010. Characterization of the proteome, diseases and evolution of the human postsynaptic density. *Nat Neurosci* **14**: 19–21.
11. **Berkel S**, **Marshall CR**, **Weiss B**, **Howe J**, et al. 2010. Mutations in the SHANK2 synaptic scaffolding gene in autism spectrum disorder and mental retardation. *Nat Genet* **42**: 489–91.
12. **Bangash MA**, **Park JM**, **Melnikova T**, **Wang D**, et al. 2011. Enhanced polyubiquitination of Shank3 and NMDA receptor in a mouse model of autism. *Cell* **145**: 758–72.
13. **Fukata Y**, **Adesnik H**, **Iwanaga T**, **Bredt DS**, et al. 2006. Epilepsy-related ligand/receptor complex LGI1 and ADAM22 regulate synaptic transmission. *Science* **313**: 1792–5.
14. **Collingridge GL**, **Kehl SJ**, **McLennan H.** 1983. Excitatory amino acids in synaptic transmission in the Schaffer collateral-commissural pathway of the rat hippocampus. *J Physiol* **334**: 33–46.
15. **Morris RG**, **Anderson E**, **Lynch GS**, **Baudry M.** 1986. Selective impairment of learning and blockade of long-term potentiation by an *N*-methyl-D-aspartate receptor antagonist, AP5. *Nature* **319**: 774–6.
16. **Mulkey RM**, **Malenka RC.** 1992. Mechanisms underlying induction of homosynaptic long-term depression in area CA1 of the hippocampus. *Neuron* **9**: 967–75.
17. **Anggono V**, **Huganir RL.** 2012. Regulation of AMPA receptor trafficking and synaptic plasticity. *Curr Opin Neurobiol*, in press, DOI: http://dx.doi.org/10.1016/j.conb.2011.12.006
18. **Malenka RC**, **Bear MF.** 2004. LTP and LTD: an embarrassment of riches. *Neuron* **44**: 5–21.
19. **Sanes JR**, **Lichtman JW.** 1999. Can molecules explain long-term potentiation? *Nat Neurosci* **2**: 597–604.
20. **Pauling L.** 1950. The place of chemistry in the integration of the sciences. *Main Curr Mod Thought* **7**: 108–11.
21. **Lee HK**, **Barbarosie M**, **Kameyama K**, **Bear MF**, et al. 2000. Regulation of distinct AMPA receptor phosphorylation sites during bidirectional synaptic plasticity. *Nature* **405**: 955–9.
22. **Malinow R**, **Schulman H**, **Tsien RW.** 1989. Inhibition of postsynaptic PKC or CaMKII blocks induction but not expression of LTP. *Science* **245**: 862–6.
23. **Derkach V**, **Barria A**, **Soderling TR.** 1999. Ca^{2+}/calmodulin-kinase II enhances channel conductance of alpha-amino-3-hydroxy-5-methyl-4-isoxazolepropionate type glutamate receptors. *Proc Natl Acad Sci USA* **96**: 3269–74.
24. **Mulkey RM**, **Endo S**, **Shenolikar S**, **Malenka RC.** 1994. Involvement of a calcineurin/inhibitor-1 phosphatase cascade in hippocampal long-term depression. *Nature* **369**: 486–8.
25. **Kameyama K**, **Lee HK**, **Bear MF**, **Huganir RL.** 1998. Involvement of apostsynaptic protein kinase A substrate in the expression of homosynaptic long-term depression. *Neuron* **21**: 1163–75.
26. **Whitlock JR**, **Heynen AJ**, **Shuler MG**, **Bear MF.** 2006. Learning induces long-term potentiation in the hippocampus. *Science* **313**: 1093–7.
27. **Liu L**, **Wong TP**, **Pozza MF**, **Lingenhoehl K**, et al. 2004. Role of NMDA receptor subtypes in governing the direction of hippocampal synaptic plasticity. *Science* **304**: 1021–4.
28. **Morishita W**, **Lu W**, **Smith GB**, **Nicoll RA**, et al. 2007. Activation of NR2B-containing NMDA receptors is not required for NMDA receptor dependent long-term depression. *Neuropharmacology* **52**: 71–6.
29. **Dick IE**, **Tadross MR**, **Liang H**, **Tay LH**, et al. 2008. A modular switch for spatial Ca^{2+} selectivity in the calmodulin regulation of CaV channels. *Nature* **451**: 830–4.

30. **Zaccolo M**, **Pozzan T.** 2002. Discrete microdomains with high concentration of cAMP in stimulated rat neonatal cardiac myocytes. *Science* **295**: 1711–5.
31. **Jurado S**, **Biou V**, **Malenka RC.** 2010. A calcineurin/AKAP complex is required for NMDA receptor-dependent long-term depression. *Nat Neurosci* **13**: 1053–5.
32. **Tunquist BJ**, **Hoshi N**, **Guire ES**, **Zhang F**, et al. 2008. Loss of AKAP150 perturbs distinct neuronal processes in mice. *Proc Natl Acad Sci USA* **105**: 12557–62.
33. **Yang Y**, **Tao-Cheng JH**, **Reese TS**, **Dosemeci A.** 2011. SynGAP moves out of the core of the postsynaptic density upon depolarization. *Neuroscience* **192**: 132–9.
34. **Jiao Y**, **Jalan-Sakrikar N**, **Robison AJ**, **Baucum AJ II**, et al. 2011. Characterization of a central Ca^{2+}/calmodulin-dependent protein kinase Ialpha/beta binding domain in densin that selectively modulates glutamate receptor subunit phosphorylation. *J Biol Chem* **286**: 24806–18.
35. **Halt AR**, **Dallapiazza RF**, **Zhou Y**, **Stein IS**, et al. 2012. CaMKII binding to GluN2B is critical during memory consolidation. *EMBO J* **31**: 1203–16.
36. **Lu J**, **Helton TD**, **Blanpied TA**, **Racz B**, et al. 2007. Postsynaptic positioning of endocytic zones and AMPA receptor cycling by physical coupling of dynamin-3 to Homer. *Neuron* **55**: 874–89.
37. **Lisman JE.** 2009. The pre/post LTP debate. *Neuron* **63**: 281–4.
38. **Huang YY**, **Li XC**, **Kandel ER.** 1994. cAMP contributes to mossy fiber LTP by initiating both a covalently mediated early phase andmacromolecular synthesis-dependent late phase. *Cell* **79**: 69–79.
39. **Weisskopf MG**, **Castillo PE**, **Zalutsky RA**, **Nicoll RA.** 1994. Mediation of hippocampal mossy fiber long-term potentiation by cyclic AMP. *Science* **265**: 1878–82.
40. **Markram H**, **Gerstner W**, **Sjostrom PJ.** 2011. A history of spike-timing dependent plasticity. *Front Synaptic Neurosci* **3**: 4.
41. **Gray EG**, **Whittaker VP.** 1962. The isolation of nerve endings from brain: an electron-microscopic study of cell fragments derived by homogenization and centrifugation. *J Anat* **96**: 79–88.
42. **Cotman CW**, **Banker G**, **Churchill L**, **Taylor D.** 1974. Isolation of postsynaptic densities from rat brain. *J Cell Biol* **63**: 441–55.
43. **Hahn CG**, **Banerjee A**, **Macdonald ML**, **Cho DS**, et al. 2009. The postsynaptic density of human postmortem brain tissues: an experimental study paradigm for neuropsychiatric illnesses. *PLoS ONE* **4**: e5251.
44. **Banker G**, **Churchill L**, **Cotman CW.** 1974. Proteins of the postsynaptic density. *J Cell Biol* **63**: 456–65.
45. **Kennedy MB**, **Bennett MK**, **Erondu NE.** 1983. Biochemical and immunochemical evidence that the ''major postsynaptic density protein'' is a subunit of a calmodulin-dependent protein kinase. *Proc Natl Acad Sci USA* **80**: 7357–61.
46. **Cho KO**, **Hunt CA**, **Kennedy MB.** 1992. The rat brain postsynaptic density fraction contains a homolog of the *Drosophila* discs-large tumor-suppressor protein. *Neuron* **9**: 929–42.
47. **Collins MO**, **Husi H**, **Yu L**, **Brandon JM**, et al. 2006. Molecular characterization and comparison of the components and multiprotein complexes in the postsynaptic proteome. *J Neurochem* **97**: 16–23.
48. **Sheng M**, **Hoogenraad CC.** 2007. The postsynaptic architecture of excitatory synapses: a more quantitative view. *Annu Rev Biochem* **76**: 823–47.
49. **Matthews BW.** 1968. Solvent content of protein crystals. *J Mol Biol* **33**: 491–7.
50. **Chen X**, **Vinade L**, **Leapman RD**, **Petersen JD**, et al. 2005. Mass of the postsynaptic density and enumeration of three key molecules. *Proc Natl Acad Sci USA* **102**: 11551–6.
51. **Cheng D**, **Hoogenraad CC**, **Rush J**, **Ramm E**, et al. 2006. Relative and absolute quantification of postsynaptic density proteome isolated from rat forebrain and cerebellum. *Mol Cell Proteomics* **5**: 1158–70.
52. **Sugiyama Y**, **Kawabata I**, **Sobue K**, **Okabe S.** 2005. Determination of absolute protein numbers in single synapses by a GFP-based calibration technique. *Nat Methods* **2**: 677–84.
53. **Trinidad JC**, **Thalhammer A**, **Specht CG**, **Lynn AJ**, et al. 2008. Quantitative analysis of synaptic phosphorylation and protein expression. *Mol Cell Proteomics* **7**: 684–96.
54. **Gold MG**, **Stengel F**, **Nygren PJ**, **Weisbrod CR**, et al. 2011. Architecture and dynamics of an A-kinase anchoring protein 79 (AKAP79) signalling complex. *Proc Natl Acad Sci USA* **108**: 6426–31.
55. **Jain A**, **Liu R**, **Ramani B**, **Arauz E**, et al. 2011. Probing cellular protein complexes using single-molecule pull-down. *Nature* **473**: 484–8.
56. **Kornau HC**, **Schenker LT**, **Kennedy MB**, **Seeburg PH.** 1995. Domain interaction between NMDA receptor subunits and the postsynaptic density protein PSD-95. *Science* **269**: 1737–40.
57. **Coghlan VM**, **Perrino BA**, **Howard M**, **Langeberg LK**, et al. 1995. Association of protein kinase A and protein phosphatase 2B with a common anchoring protein. *Science* **267**: 108–11.
58. **Kim JH**, **Liao D**, **Lau LF**, **Huganir RL.** 1998. SynGAP: a synaptic RasGAP that associates with the PSD-95/SAP90 protein family. *Neuron* **20**: 683–91.
59. **Husi H**, **Ward MA**, **Choudhary JS**, **Blackstock WP**, et al. 2000. Proteomic analysis of NMDA receptor-adhesion protein signalling complexes. *Nat Neurosci* **3**: 661–9.
60. **Husi H**, **Grant SG.** 2001. Isolation of 2000-kDa complexes of *N*-methyl-D-aspartatereceptor and postsynaptic density 95 from mouse brain. *J Neurochem* **77**: 281–91.
61. **Hardingham GE**, **Fukunaga Y**, **Bading H.** 2002. Extrasynaptic NMDARs oppose synaptic NMDARs by triggering CREB shut-off and cell death pathways. *Nat Neurosci* **5**: 405–14.
62. **Fernandez E**, **Collins MO**, **Uren RT**, **Kopanitsa MV**, et al. 2009. Targeted tandem affinity purification of PSD-95 recovers core postsynaptic complexes and schizophrenia susceptibility proteins. *Mol Syst Biol* **5**: 269.
63. **Zhou M**, **Robinson CV.** 2010. When proteomics meets structural biology. *Trends Biochem Sci* **35**: 522–9.
64. **Leitner A**, **Walzthoeni T**, **Kahraman A**, **Herzog F**, et al. 2010. Probing native protein structures by chemical cross-linking, mass spectrometry, and bioinformatics. *Mol Cell Proteomics* **9**: 1634–49.
65. **Zheng C**, **Yang L**, **Hoopmann MR**, **Eng JK**, et al. 2011. Cross-linking measurements of in vivo protein complex topologies. *Mol Cell Proteomics* **10**: M110 006841.
66. **Sharon M**, **Robinson CV.** 2007. The role of mass spectrometry in structure elucidation of dynamic protein complexes. *Annu Rev Biochem* **76**: 167–93.
67. **Chen X**, **Winters C**, **Azzam R**, **Li X**, et al. 2008. Organization of the core structure of the postsynaptic density. *Proc Natl Acad Sci USA* **105**: 4453–8.
68. **Nakagawa T**, **Futai K**, **Lashuel HA**, **Lo I**, et al. 2004. Quaternary structure, protein dynamics, and synaptic function of SAP97 controlled by L27 domain interactions. *Neuron* **44**: 453–67.
69. **Chen X**, **Nelson CD**, **Li X**, **Winters CA**, et al. 2011. PSD-95 is required to sustain the molecular organization of the postsynaptic density. *J Neurosci* **31**: 6329–38.
70. **Valtschanoff JG**, **Weinberg RJ.** 2001. Laminar organization of the NMDA receptor complex within the postsynaptic density. *J Neurosci* **21**: 1211–7.
71. **Baron MK**, **Boeckers TM**, **Vaida B**, **Faham S**, et al. 2006. An architectural framework that may lie at the core of the postsynaptic density. *Science* **311**: 531–5.
72. **Hayashi MK**, **Tang C**, **Verpelli C**, **Narayanan R**, et al. 2009. The postsynaptic density proteins Homer and Shank form a polymeric network structure. *Cell* **137**: 159–71.
73. **Racz B**, **Blanpied TA**, **Ehlers MD**, **Weinberg RJ.** 2004. Lateral organization of endocytic machinery in dendritic spines. *Nat Neurosci* **7**: 917–8.
74. **Rostaing P**, **Real E**, **Siksou L**, **Lechaire JP**, et al. 2006. Analysis of synaptic ultrastructure without fixative using high-pressure freezing and tomography. *Eur J Neurosci* **24**: 3463–74.
75. **Huang B**, **Wang W**, **Bates M**, **Zhuang X.** 2008. Three-dimensional superresolution imaging by stochastic optical reconstruction microscopy. *Science* **319**: 810–3.
76. **Betzig E**, **Patterson GH**, **Sougrat R**, **Lindwasser OW**, et al. 2006. Imaging intracellular fluorescent proteins at nanometer resolution. *Science* **313**: 1642–5.
77. **Dani A**, **Huang B**, **Bergan J**, **Dulac C**, et al. 2011. Super-resolution imaging of chemical synapses in the brain. *Neuron* **68**: 843–56.
78. **Izeddin I**, **Specht CG**, **Lelek M**, **Darzacq X**, et al. 2011. Super-resolution dynamic imaging of dendritic spines using a low-affinity photoconvertible actin probe. *PLoS ONE* **6**: e15611.
79. **Ehlers MD**, **Heine M**, **Groc L**, **Lee MC**, et al. 2007. Diffusional trapping of GluR1 AMPA receptors by input-specific synaptic activity. *Neuron* **54**: 447–60.
80. **Sobolevsky AI**, **Rosconi MP**, **Gouaux E.** 2009. X-ray structure, symmetry and mechanism of an AMPA-subtype glutamate receptor. *Nature* **462**: 745–56.
81. **Furukawa H**, **Singh SK**, **Mancusso R**, **Gouaux E.** 2005. Subunit arrangement and function in NMDA receptors. *Nature* **438**: 185–92.
82. **Wu J**, **Brown SH**, **von Daake S**, **Taylor SS.** 2007. PKA type II alpha holoenzyme reveals a combinatorial strategy for isoform diversity. *Science* **318**: 274–9.

83. **Griffith JP**, **Kim JL**, **Kim EE**, **Sintchak MD**, et al. 1995. X-ray structure of calcineurin inhibited by the immunophilin-immunosuppressant FKBP12-FK506 complex. *Cell* **82**: 507–22.
84. **Chao LH**, **Stratton MM**, **Lee IH**, **Rosenberg OS**, et al. 2011. A mechanism for tunable autoinhibition in the structure of a human Ca^{2+}/calmodulin-dependent kinase II holoenzyme. *Cell* **146**: 732–45.
85. **Terrak M**, **Kerff F**, **Langsetmo K**, **Tao T**, et al. 2004. Structural basis of protein phosphatase 1 regulation. *Nature* **429**: 780–4.
86. **Doyle DA**, **Lee A**, **Lewis J**, **Kim E**, et al. 1996. Crystal structures of a complexed and peptide-free membrane protein-binding domain: molecular basis of peptide recognition by PDZ. *Cell* **85**: 1067–76.
87. **Gold MG**, **Lygren B**, **Dokurno P**, **Hoshi N**, et al. 2006. Molecular basis of AKAP specificity for PKA regulatory subunits. *Mol Cell* **24**: 383–95.
88. **Kinderman FS**, **Kim C**, **von Daake S**, **Ma Y**, et al. 2006. A dynamic mechanism for AKAP binding to RII isoforms of cAMP-dependent protein kinase. *Mol Cell* **24**: 397–408.
89. **Li H**, **Zhang L**, **Rao A**, **Harrison SC**, et al. 2007. Structure of calcineurin-inin complex with PVIVIT peptide: portrait of a low-affinity signalling interaction. *J Mol Biol* **369**: 1296–306.
90. **Li H**, **Pink MD**, **Murphy JG**, **Stein A**, et al. 2012. Balanced interactions of calcineurin with AKAP79 regulate Ca(2+)-calcineurin-NFAT signaling. *Nat Struct Mol Biol* **19**: 337–45.
91. **Crick F.** 1988. *What Mad Pursuit: a Personal View of Scientific Discovery*. London: Penguin **1990**: p. 114–5.
92. **Schreiber A**, **Stengel F**, **Zhang Z**, **Enchev RI**, et al. 2011. Structural basis for the subunit assembly of the anaphase-promoting complex. *Nature* **470**: 227–32.
93. **Robertson HR**, **Gibson ES**, **Benke TA**, **Dell'Acqua ML.** 2009. Regulation of postsynaptic structure and function by an A-kinase anchoring protein-membrane-associated guanylate kinase scaffolding complex. *J Neurosci* **29**: 7929–43.
94. **Szklarczyk D**, **Franceschini A**, **Kuhn M**, **Simonovic M**, et al. 2011. The STRING database in 2011: functional interaction networks of proteins, globally integrated and scored. *Nucleic Acids Res* **39**: D561–D568.
95. **Berman H**, **Henrick K**, **Nakamura H**, **Markley JL.** 2007. The worldwide Protein Data Bank (wwPDB): ensuring a single, uniform archive of PDB data. *Nucleic Acids Res* **35**: D301–D303.
96. **Pettersen EF**, **Goddard TD**, **Huang CC**, **Couch GS**, et al. 2004. UCSF Chimera – a visualization system for exploratory research and analysis. *J Comput Chem* **25**: 1605–12.
97. **Winn MD**, **Ballard CC**, **Cowtan KD**, **Dodson EJ**, et al. 2011. Overview of the CCP4 suite and current developments. *ActaCrystallogr D BiolCrystallogr* **67**: 235–42.
98. **Suhre K**, **Navaza J**, **Sanejouand YH.** 2006. NORMA: a tool for flexible fitting of high-resolution protein structures into low-resolution electron microscopy-derived density maps. *Acta Crystallogr D Biol Crystallogr* **62**: 1098–100.
99. **Morange M.** 1998. *A History of Molecular Biology Cambridge Mass*. London: Harvard University Press. p. 336
100. **Kitano H**, **Funahashi A**, **Matsuoka Y**, **Oda K.** 2005. Using process diagrams for the graphical representation of biological networks. *Nat Biotechnol* **23**: 961–6.
101. **Blundell TL**, **Harrison SC**, **Stroud RM**, **Yokoyama S**, et al. 2011. Celebrating structural biology. *Nat Struct Mol Biol* **18**: 1304–16.
102. **Smith KE**, **Gibson ES**, **Dell'Acqua ML**. 2006. cAMP-dependent protein kinase postsynaptic localization regulated by NMDA receptor activation through translocation of an A-kinase anchoring protein scaffold protein. *J Neurosci* **26**: 2391–402.
103. **Kerr JM**, **Blanpied TA.** 2012. Subsynaptic AMPA receptor distribution is acutely regulated by actin-driven reorganization of the postsynaptic density. *J Neurosci* **32**: 658–73.
104. **Nowak L**, **Bregestovski P**, **Ascher P**, **Herbet A**, et al. 1984. Magnesium gates glutamate-activated channels in mouse central neurones. *Nature* **307**: 462–5.
105. **Petersen JD**, **Chen X**, **Vinade L**, **Dosemeci A**, et al. 2003. Distribution of postsynaptic density (PSD)-95 and Ca^{2+}/calmodulin-dependent protein kinase II at the PSD. *J Neurosci* **23**: 11270–8.
106. **Dell'Acqua ML**, **Faux MC**, **Thorburn J**, **Thorburn A**, et al. 1998. Membrane-targeting sequences on AKAP79 bind phosphatidylinositol-4, 5-bisphosphate. *EMBO J* **17**: 2246–60.
107. **Ye Q**, **Wang H**, **Zheng J**, **Wei Q**, et al. 2008. The complex structure of calmodulin bound to a calcineurin peptide. *Proteins* **73**: 19–27.
108. **Ghosh S**, **Matsuoka Y**, **Asai Y**, **Hsin KY**, et al. 2011. Software for systems biology: from tools to integrated platforms. *Nat Rev Genet* **12**: 821–32.
109. **Davison AP**, **Hines ML**, **Muller E.** 2009. Trends in programming languages for neuroscience simulations. *Front Neurosci* **3**: 374–80.